NANO LETTERS

2004
Vol. 4, No. 6
1089−1092

Size Dependent Femtosecond Electron Cooling Dynamics in CdSe Quantum Rods

Pingrong Yu,*,†,‡ Jovan M. Nedeljkovic,† Phil A. Ahrenkiel,† Randy J. Ellingson,† and Arthur J. Nozik*†,‡

Center for Basic Sciences, National Renewable Energy Laboratory, Golden, Colorado 80401 and Department of Chemistry and Biochemistry, University of Colorado, Boulder, Colorado 80309

Received March 28, 2004; Revised Manuscript Received April 23, 2004

ABSTRACT

Electronic relaxation dynamics of photoexcited CdSe quantum rods have been studied with femtosecond transient absorption spectroscopy. Samples with the same length, ~30 nm, but with different diameters, 2.5 and 8.0 nm, were investigated. We found that the intraband energy relaxation is about 8 times faster in the thin rods than in the thick ones. A comparison is made between relaxation dynamics in quantum rods and dots, and different relaxation mechanisms are discussed.

Carrier cooling dynamics in semiconductor nanomaterials is a very important scientific problem, with implications for many practical applications. For example, in novel quantum lasers,[1] it is critical that hot photogenerated carriers relax before photon emission; while in solar energy conversion, the efficiency could be dramatically increased if hot carriers could be utilized before they cool.[2,3] The cooling mechanism in semiconductor nanomaterials is still under intense debate.[3]

One very important recent development in semiconductor nanoscience is the ability to control the shape[4] of colloidal nanomaterials. Shape control provides more flexibility and options for the design of new materials to satisfy unique requirements. Quantum rods (QRs)[5] are of particular interest; they have thin diameters that confine carriers radially to produce quantum size effects, while the long axial dimension allows free carrier motion without significant quantum size effects. QRs have already shown many advantages compared to quantum dots (QDs), e.g., in lasing[1] and polymer−semiconductor hybrid solar cells.[6] However, only a few ultrafast spectroscopic studies of QRs are found in the literature;[1,7] they showed that QRs have different photocarrier dynamics compared to QDs. In this letter, we report dynamical studies of QR samples with the same rod length but with different diameters, using femtosecond transient absorption (TA) spectroscopy to better understand the carrier cooling dynamics in nanomaterials and the effect of shape.

CdSe QRs were prepared as described elsewhere.[8] Typically, 0.205 g of CdO was mixed with 0.893 g of tetradecylamine (TDA) and 2.903 g of trioctylphosphine oxide (TOPO). Complete dissolution of CdO takes place at elevated temperatures (>290 °C). At 320 °C and under air-free conditions, a solution containing 1.447 g of trioctylphosphine (TOP), 0.3 g of toluene, and 0.253 g of Se-TBP (tributyl phosphine) solution (25 wt.-%) was injected into the CdO solution. The reaction solution was quickly cooled to 250 °C, and after 30 min cooled further to room temperature. This procedure produces rods of 30 × 8 nm, length by diameter. To obtain 30 × 2.5 nm rods, we used the same chemical mixture but decreased the injection temperature to 255 °C, quickly cooled the reaction solution to 170 °C after three minutes, and further cooled it to room-temperature slowly. The resultant CdSe rods were cleaned after precipitation with methanol and redissolved in appropriate organic solvents (hexane, toluene). The CdSe rods were used as prepared without any size selection procedures.

Figure 1 shows TEM pictures of the two samples. The QRs in sample A are 29.7 ± 6.7 × 2.5 ± 0.4 nm, length by diameter, and in sample B are 31.2 ± 4.4 × 8.0 ± 1.1 nm. Thus the two CdSe QRs samples have about the same length but diameters differing by more than a factor of 3. The absorption spectrum of each sample (Figure 2) shows a first exciton absorption peak (noted as I) and a shoulder representing a second exciton transition at shorter wavelength (noted as II). The energy spacing between transitions I and II is 0.64 eV for sample A and 0.39 eV for sample B.

Our TA setup is based on an amplified Ti:sapphire laser (Clark-MXR, CPA-2001), operating at 989 Hz. The 775 nm

* Corresponding authors. E-mail: pingrong_yu@nrel.gov; anozik@nrel.gov.
† National Renewable Energy Laboratory.
‡ University of Colorado.

10.1021/nl049524d CCC: $27.50
Published on Web 05/08/2004

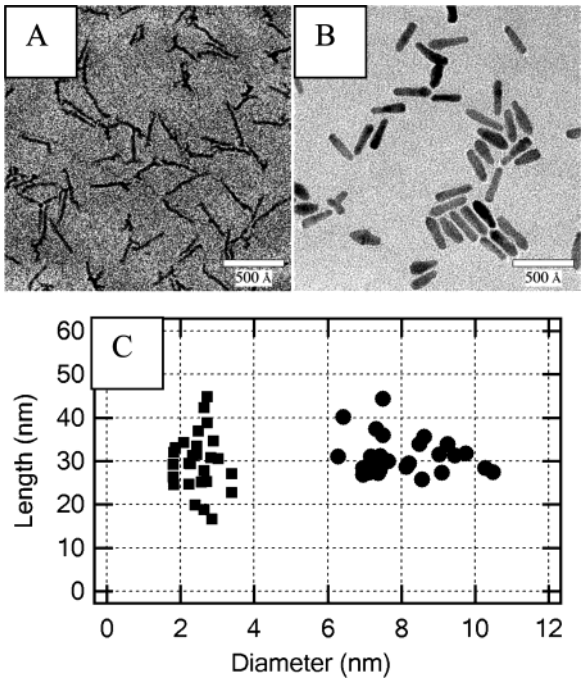

Figure 1. (A,B) TEM pictures of samples A and B, respectively. C: Size information for the two samples. Sample A (squares) contains nanorods of 29.7 ± 6.7 × 2.5 ± 0.4 nm, length by diameter, while they are 31.2 ± 4.4 × 8.0 ± 1.1 nm in sample B (circles). Nanorods in the two samples are about the same length yet different diameters.

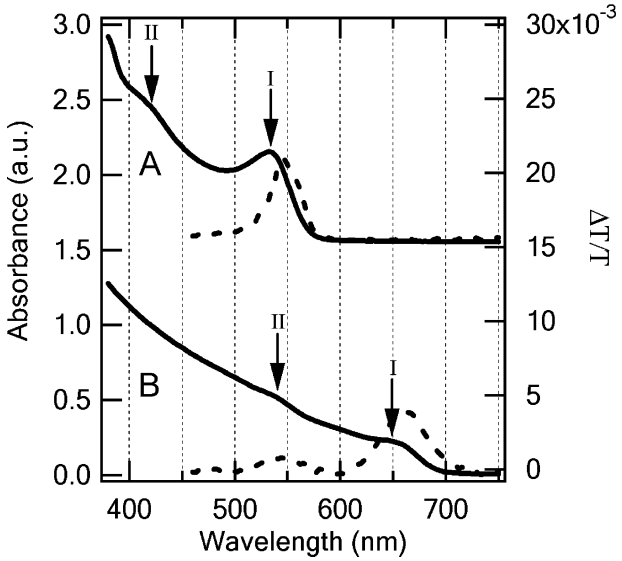

Figure 2. Absorption spectra (solid lines) and transient absorption spectra (dashed lines) at 100 ps delay after band gap pump of the two samples. The two curves on top of sample A are vertically displaced relative to the bottom two curves of B for clarity. The absorption spectrum of each sample shows a first exciton absorption peak (532 nm for A and 648 nm for B, noted as I) and a shoulder (418 nm for A and 539 nm for B, noted as II) at shorter wavelengths. The transient absorption peaks (548 nm for A and 660 nm for B) at 100 ps delay indicate photon-induced band gap absorption bleaching.

output pulsed beam is split into two parts, one to pump a TOPAS (Light Conversion) optical parametric amplifier generating a pulsed output tunable from 290 to 2600 nm, the other to pump a 2 mm sapphire window to generate probe pulses of a white light continuum that ranges from 440 to 950 nm. Probe pulses are delayed relative to the pump using an optical delay line. To eliminate directional and rotational influences on the signal, we performed the TA experiments with pump and probe polarizations at the Magic angle. The diameter of the pump beam spot is typically 450 μm, and that of the probe beam is less than 150 μm; they are measured with a 150 μm pinhole. All pump light was set to very low intensity (typically less than 1 μW) to avoid producing multiple excitons per quantum rod.

We investigate the carrier cooling dynamics in QRs, taking advantage of their resonant optical nonlinearities, which are primarily due to the carrier-induced Stark effect and to state filling effects.[9] The Stark effect results in both a shift of the optical transitions and changes in transition oscillator strengths via modification of the selection rules. State filling induces bleaching of the interband optical transitions involving populated energy states. The dashed lines in Figure 2 show band gap bleaching signals 100 ps after excitation and after the carriers have cooled. State filling effects selectively affect only populated states and dominate at longer delay times; the Stark effect universally affects all transitions and dominates at shorter delay times (<1 ps).[10] Because at low pump intensity, the transmission change ($\Delta T/T$) resulting from state filling effects is proportional to the sum of the electron and hole occupation numbers, its evolution with delay indicates that state population change with time is involved in the measurement. Here ΔT is the difference of the probe beam transmission with and without the pump, T is the transmission without the pump. However, because of the much larger effective mass and more closely spaced energy states of holes, state filling effects arise primarily from electrons. In our dynamics study we set the probe at the band gap and measure $\Delta T/T$ while changing the delay time (see inset of Figure 3A); the signal then directly reflects the electron population change at the bottom of the conduction band after the initial excitation pulse.

To best compare the cooling rates in CdSe QRs of different diameters, we excited both samples at the same resonant transition, i.e., peak II (418 nm for A and 539 nm for B), and probed their band gap bleaching (548 nm for A and 660 nm for B). The TA results are shown in Figure 3, with the red filled circles for sample A and green open circles for sample B. The rise time can be best fit to 200 fs for sample A and 1 ps for sample B. The dashed lines in Figure 3 are the pump−probe response functions of the system measured by two-photon absorption in a ZnO crystal.

The rise times above are attributed to the cooling times of the hot electrons from the excited states (represented by peak II) to the lowest exciton states (band gap). Here we define cooling time to be the mean lifetime of electrons in the original excited states, or the time needed for the electron population of the original excited states to decrease to 1/e of its initial value. To double-check the attribution of the rise time, we compared the above data with TA results pumping the samples to peak I while again probing the band gap bleaching. From Figure 3 one can see when the two

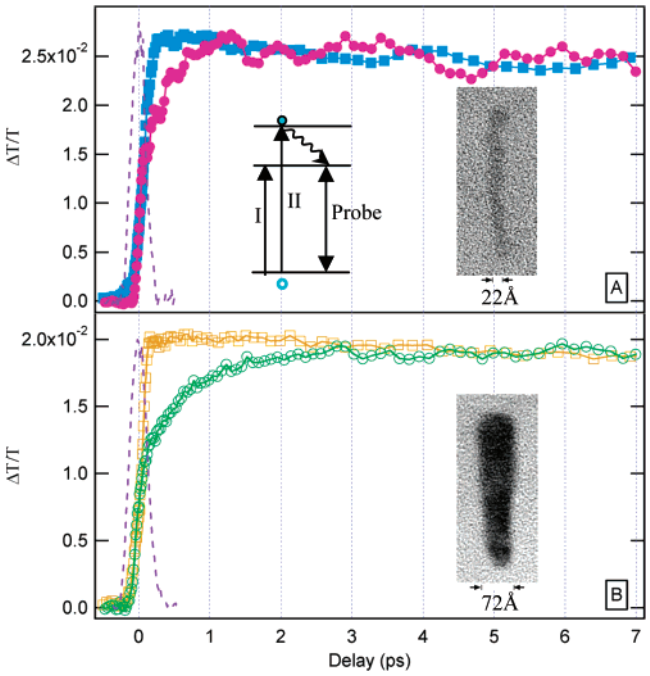

Figure 3. (A) Normalized TA results of sample A. Blue filled squares: pump = 532 nm, probe = 548 nm; red filled circles: pump = 418 nm, probe = 548 nm. Inset: TA experimental diagram (left) and TEM picture of one rod of sample A (right). (B) Normalized TA results of sample B. Yellow open squares: pump = 648 nm, probe = 660 nm; green open circles: pump = 539 nm, probe = 660 nm. Inset: TEM picture of one rod of sample B. The rise time is 200 fs for the red filled circle plot and 1 ps for the green open circle plot. Dashed lines are the setup's pump−probe response functions measured by two-photon absorption in a ZnO crystal.

sets of data are both normalized around time zero and after a few picoseconds or less, the data set for pumping at peak I has a larger magnitude than the one pumping at peak II for early delay times. This is because electrons excited to II need a longer time to cool and induce band-edge bleaching than those excited to I. In other words, the difference of the two sets of data directly reflects the cooling time from II to I. The difference lasts 1 ps for sample A and 5 ps for sample B. If we assume the cooling process from II to I is exponential, we can extract a cooling time of 200 fs for sample A and 1 ps for sample B. This matches well to our numerical fit of the rise time of the data pumping at II and probing the band gap; thus the cooling times we report are believed to be valid.

The above results translate to 3.2 and 0.39 eV/ps for the cooling rates for samples A and B, respectively. In other words, the rate of hot electron cooling in sample A is 8.2 times faster than in B. Thus, when the particle length is the same, the cooling is faster in the thinner rods. This size-dependent cooling rate is similar to that seen in QDs,[9,11] where cooling was found to be faster in smaller dots. This similarity is very interesting, because the size quantization effect and the energy level structure in dots and rods are different.

QDs confine electrons in all three dimensions, and thus the energy levels are discrete. However, in QRs, when the length exceeds the electron confinement regime, which is the case for the rods we studied here, this one-dimensional degree of freedom will induce many energy levels in the conduction and valence bands and make the energy level structure and the density of states function more like those in quantum wires.[12] The existence of additional energy states can be seen in the nonzero density of states in the tunneling spectra,[13] and also in the broad bleaching feature in transient absorption spectroscopy.[7] However, we find that these additional electronic states do not result in faster electron cooling in QRs compared to that in QDs. In fact, recent experimental results showed that the cooling in QRs is significantly slower than that in QDs.[7] From these results, together with the fact that thinner rods favor faster cooling, we can conclude that electron cooling via LO phonon emission through the additional energy levels is not the dominant process for cooling of hot electrons in QRs.

It is useful to discuss electron cooling mechanisms in QDs since they may also be applicable to QRs. If the dominant mechanism for cooling hot electrons in QDs is via emitting LO phonons, as in bulk materials, then one expects a slower cooling rate in smaller dots since the spacing of the intraband states would be larger and a phonon bottleneck would exist.[3] However, many experimental studies[9,11] showed the opposite results, so cooling by LO phonon emission is not the dominant mechanism.

Another proposed mechanism is Auger cooling, where hot electrons transfer kinetic energy to holes and the latter then cool fast because of their relatively larger effective mass and smaller intraband electronic energy level spacing. The Auger cooling mechanism can explain the experimental size dependence of cooling in QDs very well: in smaller QDs, the Coulomb attraction between electrons and holes is stronger, favoring enhanced energy transfer between them. Similarly, an Auger cooling mechanism could explain why in our results with QRs the thinner rods have a faster cooling rate; electrons and holes in 1-D confined excitons are squeezed closer together and they can exchange energy more efficiently in thinner rods than in thicker ones.

However, the Auger cooling mechanism cannot explain the results of electron cooling measurements in negatively charged QDs (no holes present)[11] or in QDs with strong hole-scavenging capping groups.[9,11,14] In these experiments, the removal of holes from the QD cores should block the Auger cooling mechanism and very slow cooling should be observed. However, while electron cooling did become slower (by about a factor of 10, to the range of 3−7 ps), the cooling was not inhibited to the extent expected in a purely Auger-dominated mechanism. A recent polaron model for electron cooling[15,16] could explain some of the experimental results, but it does not apply to nanocrystals with intraband level spacing significantly larger than twice the LO phonon energy. Thus, additional electron cooling models are needed to explain all of the results of electron cooling experiments in QDs and QRs.

Acknowledgment. This work was supported by the Office of Science, U.S. Department of Energy, Office of

Basic Energy Sciences, Division of Chemical, Geothermal, and Biosciences.

References

(1) Htoon, H.; Hollingworth, J.; Malko, A.; Dickerson, R.; Klimov, V. *Appl. Phys. Lett.* **2003**, *82*, 4776.
(2) Nozik, A. J. *Physica E* **2002**, *14*, 115.
(3) Nozik, A. J. *Annu. Rev. Phys. Chem.* **2001**, *52*, 193.
(4) Scher, E.; Manna, L.; Alivisatos, A. P. *Philos. Trans. R. Soc. London, Ser. A* **2003**, *361*, 241.
(5) Peng, X.; Manna, L.; Yang, W.; Wickham, J.; Scher, E.; Kadavanich, A.; Alivisatos, A. P. *Nature* **2000**, *404*, 59.
(6) Huynh, W.; Dittmer, J.; Alivisatos, A. P. *Science* **2002**, *295*, 2425.
(7) Mohamed, M.; Burda, C.; El-Sayed, M. *Nano Lett.* **2001**, *1*, 589.
(8) Peng, Z. A.; Peng, X. *J. Am. Chem. Soc.* **2002**, *124*, 3343.
(9) Klimov, V. *J. Phys. Chem. B* **2000**, *104*, 6112.
(10) Klimov, V.; Hunsche, S.; Kurz, H. *Phys. Rev. B* **1994**, *50*, 8110.
(11) Blackburn, J. L.; Ellingson, R. J.; Micic, O. I.; Nozik, A. J. *J. Phys. Chem. B* **2003**, *107*, 102.
(12) Alivisatos, A. P. *J. Phys. Chem.* **1996**, *100*, 13226.
(13) Banin, U.; Millo, O. *Annu. Rev. Phys. Chem.* **2003**, *54*, 465.
(14) Guyot-Sionnest, P.; Shim, M.; Matranga, C.; Hines, M. *Phys. Rev. B* **1999**, *60*, R2181.
(15) Heitz, R.; Schliwa, A.; Bimberg, D. *Phys. Status Solidi B* **2003**, *237*, 308.
(16) Verzelen, O.; Ferreira, R.; Bastard, G. *Phys. Rev. B* **2000**, *62*, R4809. Verzelen, O.; Ferreira, R.; Bastard, G. *Phys. Rev. Lett.* **2002**, *88*, 146803. Verzelen, O.; Ferreira, R.; Bastard, G. *Phys. Rev. B* **2002**, *66*, 081308(R).

NL049524D